# Topological Casimir effect in a quantum LC circuit: Real-time dynamics

Yuan Yao and Ariel R. Zhitnitsky

*Department of Physics and Astronomy, University of British Columbia,*
*Vancouver, British Columbia V6T 1Z1, Canada*

We study novel contributions to the partition function of the Maxwell system defined on a small compact manifold $\mathbb{M}$ with nontrivial mappings $\pi_1[U(1)] \cong \mathbb{Z}$. These contributions cannot be described in terms of conventional physical propagating photons with two transverse polarizations and instead emerge as a result of tunneling transitions between topologically different but physically identical vacuum winding states. We argue that if the same system is considered in the background of a small external time-dependent electromagnetic field, then real physical photons will be emitted from the vacuum, similar to the dynamical Casimir effect where photons are radiated from the vacuum due to time-dependent boundary conditions. The fundamental technical difficulty for such an analysis is that the radiation of physical photons on mass shell is inherently a real-time Minkowskian phenomenon while the vacuum fluctuations interpolating between topological $|k\rangle$ sectors rest upon a Euclidean instanton formulation. We overcome this obstacle by introducing auxiliary topological fields, which allows for a simple analytical continuation between Minkowski and Euclidean descriptions, and develop a quantum mechanical technique to compute these effects. We also propose an experimental realization of such small effects using a microwave cavity with appropriate boundary conditions. Finally, we comment on the possible cosmological implications of this effect.

## I. INTRODUCTION AND MOTIVATION

It has been recently argued [1–5] that some novel terms in the partition function emerge when pure Maxwell theory is defined on a small compact manifold. These terms are not related to the propagating photons with two transverse physical polarizations, which are responsible for the conventional Casimir effect (CE) [6]. Rather, they occur as a result of tunneling events between topologically different but physically identical $|k\rangle$ topological sectors. While such contributions are irrelevant in Minkowski space-time $\mathbb{R}_{1,3}$, they become important when the system is defined on certain small compact manifolds. Without loss of generality, consider a manifold $\mathbb{M}$ which has at least one nontrivial direct factor of the fundamental group, e.g., $\pi_1[U(1)] \cong \mathbb{Z}$. The topological sectors $|k\rangle$, which play a key role in our discussions, arise precisely from the presence of such nontrivial mappings for the $U(1)$ Maxwell gauge theory. The corresponding physically observable phenomenon has been termed the topological Casimir effect (TCE).

In particular, it has been explicitly shown in Ref. [1] that these novel terms in the topological portion of the partition function $\mathcal{Z}_{\text{top}}$ lead to a fundamentally new contribution to the Casimir vacuum pressure that appears as a result of tunneling events between topological sectors $|k\rangle$. Furthermore, $\mathcal{Z}_{\text{top}}$ displays many features of topologically ordered systems, which were initially introduced in the context of condensed matter (CM) systems (see recent reviews [7–11]): $\mathcal{Z}_{\text{top}}$ demonstrates the degeneracy of the system, which can only be described in terms of nonlocal operators [2]; the infrared physics of the system can be studied in terms of nonpropagating auxiliary topological fields [3], analogous to how a topologically ordered system can be analyzed in terms of the Berry connection (also an emergent rather than fundamental field), and the corresponding expectation value of the auxiliary topological field determines the phase of the system. In fact, this technical trick of describing the system in terms of auxiliary fields will play a key role in our present discussions.

As we review in Sec. II A, the relevant vacuum fluctuations which saturate the topological portion of the partition function $\mathcal{Z}_{\text{top}}$ are formulated in terms of topologically nontrivial boundary conditions. Classical instantons formulated in Euclidean space-time satisfy the periodic boundary conditions up to a large gauge transformation and provide topological magnetic instanton fluxes in the $z$-direction. These integer magnetic fluxes describe the tunneling transitions between physically identical but topologically distinct $|k\rangle$ sectors. Precisely, these field configurations generate an extra Casimir vacuum pressure in the system.

What happens to this complicated vacuum structure when the system is placed in the background of a constant external magnetic field $B_{\text{ext}}^z$? The answer is known [1]: the corresponding partition function $\mathcal{Z}_{\text{top}}$ as well as all observables, including the topological contribution to the Casimir pressure, are highly sensitive to small magnetic fields and demonstrate $2\pi$ periodicity with respect to the external magnetic flux represented by the parameter $\theta_{\text{eff}} \equiv eSB_{\text{ext}}^z$ where $S$ is the $xy$ area of the system $\mathbb{M}$. This sensitivity to the external magnetic field is a result of the quantum interference of the external field with the topological

065018-1

quantum fluctuations. Alternatively, one can see this as resulting from a small but nontrivial overlap between the conventional Fock states, constructed by perturbative expansions around each $|k\rangle$ sector, and the true energy eigenstates of the theory, which are only attainable in a nonperturbative computation that takes the tunneling into account. This strong "quantum" sensitivity of the TCE should be contrasted with conventional Casimir forces which are practically unaltered by any external field due to the strong suppression $\sim B_{\text{ext}}^2/m_e^4$ (see Ref. [1] for the details).

What happens when the external E&M field depends on time? It has been argued in Refs. [4,5] that the corresponding systems will radiate real physical photons with transverse polarizations. However, the arguments of Refs. [4,5] were based on purely classical considerations at small frequencies $\omega \to 0$ of the external fields. The main goal of the present work is to the study the quantum dynamics of the topological vacuum transitions between $|k\rangle$ states in the presence of a *rapidly time-varying* external E&M field.

The fundamental technical difficulty for such an analysis is that the radiation of real physical particles on mass shell is inherently formulated in *Minkowski* space-time with a well-defined Hilbert space of asymptotic states. At the same time, the vacuum fluctuations ("instanton fluxes") interpolating between the topological $|k\rangle$ sectors and saturating the path integral are fundamentally formulated in *Euclidean* space-time.[1]

We overcome this obstacle by introducing auxiliary topological fields to effectively describe the tunneling transitions computed in Euclidean space-time. These auxiliary fields can be analytically continued to Minkowski space-time. After making the connection between the auxiliary topological fields and the Minkowski observables, we proceed using conventional Minkowski-based techniques, including the construction of the creation and annihilation operators, coherent states, the appropriate Hamiltonian describing the coupling of the microwave cavity to the system, etc.

Our presentation is organized as follows. In Sec. II, we review the relevant elements of the system including the formulation of the magnetic (II A) and electric (II B) instanton fluxes. In Sec. III, we construct the dipole moment operators (electric and magnetic types) using our auxiliary fields continued to Minkowski space-time. In Sec. IV, we formulate the problem of radiation in proper quantum mechanical terms by identifying the quantum

"states" of the system and studying the quantum matrix elements between them. In Sec. V, we discuss quantum transitions in the system in a cavity in the presence of a time-dependent external E&M field. In the concluding section, Sec. VI, we speculate that the same "nondispersive" type of vacuum energy (which cannot be expressed in terms of any propagating degrees of freedom and is the subject of the present work) might be responsible for the de Sitter phase of our Universe, where the vacuum energy plays a crucial role in its evolution.

## II. TOPOLOGICAL PARTITION FUNCTION. EUCLIDEAN PATH INTEGRAL FORMULATION

Our goal here is to review the Maxwell system defined on a Euclidean 4-manifold $\mathbb{I}^1 \times \mathbb{I}^1 \times \mathbb{S}^1 \times \mathbb{S}^1$ with sizes $L_1 \times L_2 \times L_3 \times \beta$ in the respective directions. This construction provides the infrared regularization of the system, which plays a key role in the proper treatment of the topological terms related to tunneling events between topologically distinct but physically identical $|k\rangle$ sectors. We start in Sec. II A with the construction of the magnetic instanton fluxes considered in Ref. [1] and continue in Sec. II B with the electric instanton fluxes considered in Ref. [5]. The construction of the respective instantons (1) and (9) has been discussed in the earlier works [1,5] and even earlier in the original studies of the Schwinger model in two dimensions [12,13], so we leave a review of the relevant details to Appendix A. Discussions on how these instanton fluxes can be generated in experiment with suitable boundary conditions can be found in Appendix B.

### A. Magnetic-type instantons

In what follows, we simplify our analysis by considering a clear case with topological winding sectors $|k\rangle$ in the $z$-direction only. This simplification can be justified with the geometry $L_1, L_2 \gg L_3, \beta$, similar to the construction of the conventional CE. In this case, our system resembles the 2D Maxwell theory in Ref. [1] by dimensional reduction: taking a slice of the four-dimensional (4D) system in the $xy$-plane will yield precisely the topological features of the 2D torus. With this geometry, the dominant classical instanton configurations that describe tunneling transitions can be written as

$$A_{\text{top}}^\mu = \left(0, -\frac{\pi k}{eL_1L_2}x_2, \frac{\pi k}{eL_1L_2}x_1, 0\right), \qquad (1)$$

where $k$ is the winding number that labels the topological sector.

This classical instanton configuration satisfies the periodic boundary conditions up to a large gauge transformation and provides a topological magnetic instanton flux in the $z$-direction:

---

[1]This problem is not specific to our system. Rather, it is a quite common problem when the path integrals are performed in Euclidean space-time, but the relevant physical questions are formulated in Minkowski terms. In particular, the problem is well known in QCD lattice simulations with conventional Euclidean formulations. All questions on nonequilibrium dynamics and particle production represent challenges for the QCD lattice community.

$$\vec{B}_{\text{top}} = \vec{\nabla} \times \vec{A}_{\text{top}} = \left(0, 0, \frac{2\pi k}{eL_1 L_2}\right),$$

$$\Phi = e \int dx_1 dx_2 B^z_{\text{top}} = 2\pi k. \qquad (2)$$

The Euclidean action of the system is quadratic and has the form

$$\frac{1}{2} \int d^4 x \{\vec{E}^2 + (\vec{B} + \vec{B}_{\text{top}} + \vec{B}_{\text{ext}})^2\}, \qquad (3)$$

where $\vec{E}$ and $\vec{B}$ are the dynamical quantum fluctuations of the gauge field and $\vec{B}_{\text{ext}}$ is classical external magnetic field.

As discussed in detail in Ref. [1], the quantum fluctuations of the gauge field decouple from the topological and external fields, allowing us to arrive at a simple expression for the topological partition function,

$$\mathcal{Z}_{\text{top}}(\tau, \theta_{\text{eff}}) = \sqrt{\pi \tau} \sum_{k \in \mathbb{Z}} \exp\left[-\pi^2 \tau \left(k + \frac{\theta_{\text{eff}}}{2\pi}\right)^2\right], \qquad (4)$$

where

$$\tau \equiv 2\beta L_3 / e^2 L_1 L_2 \qquad (5)$$

is a dimensionless system size parameter and the effective theta parameter $\theta_{\text{eff}} \equiv eL_1 L_2 B^z_{\text{ext}}$ is defined in terms of the external magnetic field $B^z_{\text{ext}}$. Applying the Poisson summation formula leads to the dual expression

$$\mathcal{Z}_{\text{top}}(\tau, \theta_{\text{eff}}) = \sum_{n \in \mathbb{Z}} \exp\left[-\frac{n^2}{\tau} + in \cdot \theta_{\text{eff}}\right]. \qquad (6)$$

Equation (6) justifies our notation for the effective theta parameter $\theta_{\text{eff}}$ as it enters the partition function in combination with integer $n$. One should emphasize that the $n$ in the dual representation (6) is not the integer magnetic flux $k$ defined in Eq. (2). Furthermore, the $\theta_{\text{eff}}$ parameter which enters (4), (6) is not the fundamental $\theta$ parameter normally introduced into the Lagrangian in front of the $\vec{E} \cdot \vec{B}$ operator. Rather, $\theta_{\text{eff}}$ should be understood as an effective parameter representing the construction of the $|\theta_{\text{eff}}\rangle$ state for each slice with nontrivial $\pi_1[U(1)]$ in the 4D system. In fact, there are three such $\theta^{M_i}_{\text{eff}}$ parameters representing different slices of the 4-torus and their corresponding external magnetic fluxes. There are similarly three $\theta^{E_i}_{\text{eff}}$ parameters representing the external electric fluxes (in Euclidean space-time) as discussed in Ref. [2], such that the total number of $\theta$ parameters classifying the system is six, in agreement with the total number of hyperplanes in four dimensions.[2]

To study the magnetic response of the system under the influence of an external magnetic field, we differentiate with respect to the external magnetic field to obtain the induced magnetic field

$$\langle B_{\text{ind}} \rangle = -\frac{1}{\beta V} \frac{\partial \ln \mathcal{Z}_{\text{top}}}{\partial B_{\text{ext}}} = -\frac{e}{\beta L_3} \frac{\partial \ln \mathcal{Z}_{\text{top}}}{\partial \theta_{\text{eff}}}$$

$$= \frac{\sqrt{\tau \pi}}{\mathcal{Z}_{\text{top}}} \sum_{k \in \mathbb{Z}} \left(B_{\text{ext}} + \frac{2\pi k}{eL_1 L_2}\right) \exp\left[-\tau \pi^2 \left(k + \frac{\theta_{\text{eff}}}{2\pi}\right)^2\right]. \qquad (7)$$

This induced magnetic field can also be interpreted as a magnetic dipole moment,

$$\langle m_{\text{ind}} \rangle = -\langle B_{\text{ind}} \rangle L_1 L_2 L_3$$

$$= -\frac{\sqrt{\tau \pi}}{\mathcal{Z}_{\text{top}}} L_3 \sum_{k \in \mathbb{Z}} \frac{\theta_{\text{eff}} + 2\pi k}{e} \exp\left[-\tau \pi^2 \left(k + \frac{\theta_{\text{eff}}}{2\pi}\right)^2\right]. \qquad (8)$$

## B. Electric-type instantons

To study the electric instanton fluxes, we consider two parallel conducting plates which form the boundary in the $z$-direction, endowing the system with the geometry of a small quantum capacitor that has plate area $L_1 \times L_2$ and separation $L_3$ at an ambient temperature of $T = 1/\beta$. These two plates are connected by an external wire to enforce the periodic boundary conditions (up to large gauge transformations) in the $z$-direction, and so the system can be viewed as a quantum LC circuit where the external wire forms an inductor L. The quantum vacuum between the plates (where the tunneling transitions occur) represents the object of our studies.

The classical instanton configuration in Euclidean space-time which describes tunneling transitions between the topological sectors $|k\rangle$ can be represented as follows,

$$A^\mu_{\text{top}}(t) = \left(0, 0, 0, \frac{2\pi k}{eL_3 \beta} t\right)$$

$$A^3_{\text{top}}(\beta) = A^3_{\text{top}}(0) + \frac{2\pi k}{eL_3}, \qquad (9)$$

where $k$ is the winding number that labels the topological sector and $t$ is the Euclidean time. This classical instanton configuration satisfies the periodic boundary conditions up to a large gauge transformation and produces a topological electric instanton flux in the $z$-direction:

$$\vec{E}_{\text{top}} = \dot{\vec{A}}_{\text{top}} = \left(0, 0, \frac{2\pi k}{eL_3 \beta}\right). \qquad (10)$$

This construction of these electric-type instantons is in fact much closer (in comparison with the magnetic instantons

---

[2]Since it is not possible to have a 3D spatial torus without embedding it in 4D spatial space, the corresponding construction where all six possible types of fluxes are generated represents a purely academic interest.

reviewed in the previous section, Sec. II A) to the Schwinger model on a circle where the relevant instanton configurations were originally constructed [12,13]. The Euclidean action of the system takes the form

$$\frac{1}{2} \int d^4x \{ (\vec{E} + \vec{E}_{top} + \vec{E}_{ext})^2 + \vec{B}^2 \}, \quad (11)$$

where, as in the magnetic case, $\vec{E}$ and $\vec{B}$ are the dynamical quantum fluctuations of the gauge field, $\vec{E}_{top}$ is the topological instanton field, and $\vec{E}_{ext}$ is a classical external field.

Unlike magnetic fields, which remain the same under analytic continuation between Euclidean and Minkowski space-times, an electric field acquires an additional factor of $i$ as it involves the zeroth component of 4-vectors, i.e., $E_z = \partial_0 A_z - \partial_z A_0$. A detailed treatment is given in Ref. [5], and here we only state the final expressions for the partition function,

$$\mathcal{Z}_{top}(\eta, \theta_{eff}^E) = \sum_{k \in \mathbb{Z}} \exp\left[ -\pi^2 \eta \left( k + \frac{\theta_{eff}^E}{2\pi} \right)^2 \right], \quad (12)$$

for a Euclidean source $\theta_{eff}^E$ and

$$\bar{\mathcal{Z}}_{top}(\eta, \theta_{eff}^M) = \sum_{k \in \mathbb{Z}} \exp\left[ -\eta (\pi^2 k^2 + i\pi k \theta_{eff}^M) \right] \quad (13)$$

for a Minkowski source,

$$\theta_{eff}^M = e L_3 \beta E_{ext}^{Mink} = -i \theta_{eff}^E. \quad (14)$$

We have used the dimensionless system size parameter

$$\eta \equiv \frac{2 L_1 L_2}{e^2 \beta L_3}. \quad (15)$$

Our interpretation in this case remains the same: in the presence of a physical external electric field $E_{ext}^{Mink}$ represented by the complex source $\theta_{eff}^E$, the path integral (12) is saturated by the Euclidean configurations (10) describing physical tunneling events between the topological sectors $|k\rangle$.

Now, one can compute the induced Minkowski-space electric field and dipole moment in response to the external source $\theta_{eff}^M$ by differentiating the partition function (13) with respect to $E_{ext}^{Mink}$:

$$\langle E_{ind}^{Mink} \rangle = -\frac{1}{\beta V} \frac{\partial \ln \bar{\mathcal{Z}}_{top}}{\partial E_{ext}^{Mink}} = -\frac{e}{L_1 L_2} \frac{\partial \ln \bar{\mathcal{Z}}_{top}}{\partial \theta_{eff}^M}$$
$$= \frac{1}{\bar{\mathcal{Z}}_{top}} \sum_{k \in \mathbb{Z}} \frac{2\pi k}{e L_3 \beta} e^{-\eta \pi^2 k^2} \sin[\pi k \eta \theta_{eff}^M]. \quad (16)$$

The expectation value for the electric dipole moment can be competed in complete analogy with magnetic case (8), and it is given by

$$\langle p_{ind}^{Mink} \rangle = -\langle E_{ind}^{Mink} \rangle L_1 L_2 L_3$$
$$= -\frac{1}{\bar{\mathcal{Z}}_{top}} \sum_{k \in \mathbb{Z}} \frac{2\pi k L_1 L_2}{e\beta} e^{-\eta \pi^2 k^2} \sin(\pi k \eta \theta_{eff}^M). \quad (17)$$

## C. Classical dipole radiation

Although (8) and (17) have been derived assuming static external magnetic and electric fields, these expressions still hold when the external fields vary slowly compared to all relevant time scales of the system. In this case, the corresponding dipole moments $\langle m_{ind}(t) \rangle$ and $\langle p_{ind}^{Mink}(t) \rangle$ also take on time dependence in response to semiclassical time-dependent external sources as (8) and (17) suggest. Hence, one can invoke the laws of classical electrodynamics to study the magnetic and electric dipole radiation as a result of this time dependence. The radiation intensity is given by the classical expressions

$$dI^M(t) = \langle \dddot{m}_{ind}(t) \rangle^2 \frac{\sin^2 \theta}{16\pi^2 c^3} d\Omega,$$
$$dI^E(t) = \langle \dddot{p}_{ind}^{Mink}(t) \rangle^2 \frac{\sin^2 \theta}{16\pi^2 c^3} d\Omega, \quad (18)$$

while the total radiated power assumes the classical form

$$I^M(t) = \frac{1}{6\pi c^3} \langle \dddot{m}_{ind}(t) \rangle^2,$$
$$I^E(t) = \frac{1}{6\pi c^3} \langle \dddot{p}_{ind}^{Mink}(t) \rangle^2 \quad (19)$$

for the magnetic and electric systems respectively. If one is to compute the average intensity $\langle I(t) \rangle$ over a cycle assuming conventional periodic oscillation $\sim \cos(\omega t)$ for the field, one gets

$$\langle I^M \rangle = \frac{\omega^4}{12\pi c^3} \langle m_{ind} \rangle^2, \qquad \langle I^E \rangle = \frac{\omega^4}{12\pi c^3} \langle p_{ind}^{Mink} \rangle^2. \quad (20)$$

A few comments are in order. First, Eqs. (18) and (19) make the important statement that the system emits physical photons from the vacuum in the presence of time-dependent external fields, in close analogy with the dynamical Casimir effect (DCE). Its difference from the conventional DCE [14–16] is that the radiation from the vacuum in our system is not due to the conversion of virtual to real photons, as illustrated in the top panel of Fig. 1. Rather, it occurs as a result of tunneling events between topologically different but physically identical vacuum winding states in a time-dependent background, and the physical photons here are emitted from these instantonlike configurations describing the tunneling transitions as illustrated in the bottom panel of Fig. 1.

Second, the magnetic dipole radiation $\sim \langle \dddot{m}_{ind}(t) \rangle^2$ can be easily understood in terms of topological nondissipating currents flowing along the ring [4], while the electric dipole
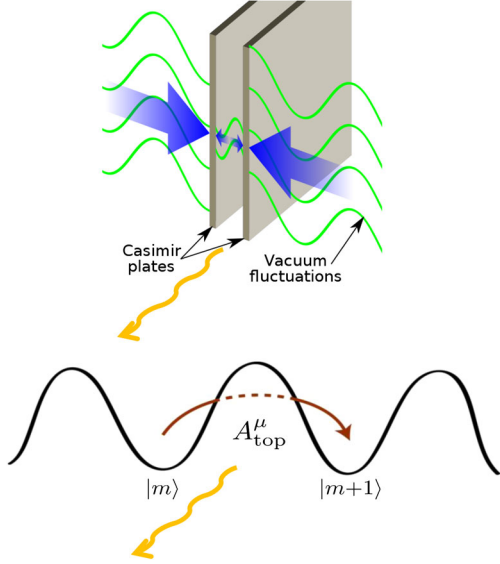
FIG. 1. An illustration of the mechanism of photon emission in the conventional DCE (top) and in the TCE or Maxwell system on a compact manifold (bottom). In the conventional DCE, the accelerating Casimir plates turn some of the virtual photons into real on-shell propagating photons which leave the system. In the case of the TCE, the tunneling transitions between infinitely degenerate vacuum winding states $|m\rangle$ are represented by instanton solutions $A_{\text{top}}^\mu$. These instanton configurations cannot be expressed in terms of physical transverse propagating E&M fields. Precisely, these topological configurations are eventually responsible for the emission of real photons in a time-dependent background; see Secs. IV and V for details.

radiation $\langle \ddot{p}_{\text{ind}}^{\text{Mink}}(t)\rangle^2$ can be understood in terms of fluctuating surface charges on the capacitor plates [5]. When the external field fluctuates, the induced nondissipating currents and surface charges follow suit. This obviously leads to the radiation of real photons as formulas (18) and (19) imply, which we call the nonstationary TCE. One should emphasize that the interpretation of the TCE (as well as nonstationary TCE, which is the subject of the present work) in terms of topological nondissipating currents and topological surface charges is the consequential, rather than fundamental, explanation. The fundamental explanation is still the instantons tunneling between the topological sectors, which occur in the system even when topological boundary currents and charges are not generated (for example, in the absence of external fields).

Finally, one should note that the above analysis of dipole radiation is purely classical; the induced dipole moments (8) and (17) are treated as classical dipoles and then varied in the semiclassical limit [such that the expressions (8) and (17) remain valid] to yield electromagnetic radiation.

The new contribution of this paper will be presented in the following sections, where we develop quantum mechanical machinery with which to study the emission of photons from the topological vacuum ($\mathcal{TV}$). This goal calls for a transition from the classical description (18), (19)

of emission in terms of dipole expectation values $\langle m_{\text{ind}}(t)\rangle$ and $\langle p_{\text{ind}}^{\text{Mink}}(t)\rangle$ to a Minkowski description based on quantum mechanical operators, quantum states, and transition matrix elements. We already mentioned the fundamental obstacle in developing such a technique; see footnote 1 and the corresponding paragraph. Formulas (18) and (19) will serve as the consistency check between the classical and quantum descriptions; it will provide some confidence that the quantum mechanical description (based on auxiliary topological fields developed in the next sections) reproduces the classical formulas (18) and (19) in the low frequency limit, as it should according to the correspondence principle.

## III. DIPOLE MOMENT OPERATORS

In this section, we use auxiliary fields to construct dipole moment operators in terms of quantum mechanical operators. These operators can be analytically continued to Minkowski space-time. They will play a crucial role in Sec. V where we study the quantum transitions in the system using quantum mechanical Hilbert states formulated in Minkowski space-time.

The expectation values for the induced electric field and dipole moment in Eqs. (16) and (17) were calculated in the Euclidean path integral approach at nonzero temperature $\beta^{-1}$. In what follows, we wish to formulate the topological features of our system using topological auxiliary fields and topological action. This technique is well known to the particle physics and CM communities. In particular, it was exploited in Ref. [17] for the Higgs model in the CM context and in Ref. [18] for the so-called weakly coupled deformed QCD. In the present context of the Maxwell system, this technique was developed in Ref. [3], and we follow the notations from that paper.

We first illustrate how to obtain the dipole moment operator for the magnetic system reviewed in Sec. II A, as it avoids the potentially confusing analytic continuation between Minkowski and Euclidean space-times. The same procedure can then be easily applied to the electric case reviewed in Sec. II B.

### A. Magnetic dipole moment

We follow Ref. [3] and insert in the original path integral (4) the following delta functional,

$$\delta[B^z - \epsilon^{zjk}\partial_j a_k(x)]$$
$$\sim \int \mathcal{D}b_z \exp\left[i\int d^4x\, b_z(x)(B^z - \epsilon^{zjk}\partial_j a_k(x))\right], \quad (21)$$

where $j$, $k = 1$, 2. Here, $B^z$ is treated as the original magnetic field operator entering the action (3), including both the classical $k$-instantons and the quantum fluctuations around them. Therefore, we treat $B^z$ as fast degrees of freedom. In comparison, the auxiliary fields $a_k(x)$ and

$b_z(x)$ should be considered slow-varying external sources that effectively describe the large distance physics which results from tunneling transitions. We proceed by summing over all instanton configurations as before and integrating out the original fast degrees of freedom in the presence of the slow fields $a_k(x)$ and $b_z(x)$. The effective Lagrangian can then be expressed in terms of these auxiliary fields.

Fortunately, the derivations can be performed as before since the Lagrange multiplier field $b_z(x)$ enters (21) in exactly the same manner in which the external magnetic field $B_{ext} \sim \theta_{eff}$ enters the action (3). Therefore, we arrive at

$$\mathcal{Z}_{top} = \sum_{k \in \mathbb{Z}} \sqrt{\pi\tau} \int \mathcal{D}a\mathcal{D}b_z \exp\left[-\int d^4x \mathcal{L}\right]$$

$$\mathcal{L} = \frac{2\pi^2}{e^2 L_1^2 L_2^2}\left(k + \frac{\theta_{eff} - i\phi(x)}{2\pi}\right)^2 + \mathcal{L}_{top}$$

$$\mathcal{L}_{top} = ib_z(x)\epsilon^{zjk}\partial_j a_k(x), \tag{22}$$

where $\phi(x) \equiv eL_1 L_2 b_z(x)$. One can see from (22) that the topological term $\mathcal{L}_{top}$ is explicitly generated in this effective description. This term has Chern-Simons structure, which normally appears in many similar CM commutations (see, e.g., Refs. [17,19]), and one should therefore anticipate a number of topological phenomena as a result of this Chern-Simons structure. Furthermore, one can show [3] that the auxiliary field $a_i(x)$ written in momentum space $a_i(\mathbf{k})$ strongly resembles Berry's connection $\mathcal{A}_i(\mathbf{k})$ in CM physics.[3]

The integration over $b_z$ is Gaussian and can be explicitly executed with the result

$$\mathcal{Z}_{top} = \sum_{k \in \mathbb{Z}} \sqrt{\pi\tau} \int \mathcal{D}a \exp\left[-\int d^4x \mathcal{L}\right]$$

$$\mathcal{L} = -\frac{1}{2}(\epsilon^{zjk}\partial_j a_k(x))^2 + \frac{2\pi k + \theta_{eff}}{eL_1 L_2}(\epsilon^{zjk}\partial_j a_k(x)). \tag{23}$$

A few comments are in order. First, the negative sign in Eq. (23) should not be considered as any inconsistency or violation of unitarity. Indeed, the field $a_k(x)$ is an auxiliary nonpropagating field introduced into the system to simplify the analysis, and any observable could be computed without it. Instead, this field should be considered as a saddle point saturating the Euclidean partition function $\mathcal{Z}_{top}$ in the path integral approach.[4]

Second, the $[-\epsilon^{zjk}\partial_j a_k(x)]$ term in the above Lagrangian couples to both the instanton field expressed in terms of $k$ fluxes and the external field formulated in terms of $\theta_{eff}$. The physical meaning of this operator can be easily understood by noticing that it enters the Lagrangian precisely like a magnetic dipole moment density couples to the external magnetic field. Therefore, we identify $[-\epsilon^{zjk}\partial_j a_k(x)]$ with the magnetization of the system.

To confirm this conjecture, we should compute the expectation value of $[-\epsilon^{zjk}\partial_j a_k(x)]$ to reproduce the magnetic dipole moment derived in the Euclidean path integral approach (8). This task can be easily performed because the integration over $\partial_j a_k(x)$ is Gaussian and can be carried out by a conventional change of variables,

$$\epsilon^{zjk}\partial_j a_k'(x) = \epsilon^{zjk}\partial_j a_k(x) - \frac{2\pi k + \theta_{eff}}{eL_1 L_2}, \tag{24}$$

after which the Lagrangian becomes

$$\mathcal{L} = -\frac{1}{2}(\epsilon^{zjk}\partial_j a_k'(x))^2 + \frac{1}{2}\left(\frac{2\pi k + \theta_{eff}}{eL_1 L_2}\right)^2. \tag{25}$$

The expectation value of $[-\epsilon^{zjk}\partial_j a_k(x)]$ is then given by

$$\langle m_{ind}\rangle = \langle[-\epsilon^{zjk}\partial_j a_k(x)]\rangle V$$

$$= \frac{\sum_{k \in \mathbb{Z}} \int \mathcal{D}a e^{-\int d^4x \mathcal{L}}\left(-\epsilon^{zjk}\partial_j a_k'(x) - \frac{2\pi k + \theta_{eff}}{eL_1 L_2}\right)V}{\sum_{k \in \mathbb{Z}} \int \mathcal{D}a e^{-\int d^4x \mathcal{L}}}$$

$$= -L_3 \frac{\sum_{k \in \mathbb{Z}}(\frac{\theta_{eff} + 2\pi k}{e})\exp[-\tau\pi^2(k + \frac{\theta_{eff}}{2\pi})^2]}{\sum_{k \in \mathbb{Z}}\exp[-\tau\pi^2(k + \frac{\theta_{eff}}{2\pi})^2]}. \tag{26}$$

Equation (26) exactly reproduces our previous expectation value of the magnetic dipole moment (8), thereby confirming the identification of the operator $[-\epsilon^{zjk}\partial_j a_k(x)]$ with the magnetization of the system.

We would like to mention here that this identification should not surprise the reader. Indeed, it has been previously argued [3] that the auxiliary field can be thought of

---

[3]In fact, one can argue that the auxiliary fields in our framework play the same role as Berry's connection in CM physics. In particular, as it is known, Berry's phase in CM systems effectively describes the variation of the $\theta$ parameter $\theta \rightarrow \theta - 2\pi P$ as a result of the coherent influence of strongly interacting fermions that polarize the system, i.e., $P = \pm 1/2$; see, e.g., Ref. [19]. Our auxiliary fields essentially describe the same physics. Therefore, it is not a surprise that the induced dipole moment $m_{ind}$, to be discussed below, can be explicitly expressed in terms of these auxiliary fields.

[4]In many respects, this negative sign in Eq. (23) resembles the negative sign for the so-called Veneziano ghost in the course of the resolution of the $U(1)_A$ problem in QCD; see Ref. [18] for references and details in the given context. One can explicitly see from the computations in Ref. [18] how the negative kinetic term for the Veneziano ghost is generated due to tunneling transitions between different topological sectors in very much the same way as it occurs in our system represented by the effective Lagrangian (23). Precisely this "wrong sign" in the effective Lagrangian might be a key element in understanding the new type of cosmological vacuum energy known as the dark energy; see comments in the concluding section, Sec. VI.

as Berry's connection.[5] The polarization properties of a CM system can be computed in terms of Berry's connection $\mathcal{A}_i(\mathbf{k})$ and Berry's curvature; see footnote 3 with relevant references. In our case, the magnetization of the system is also expressed in terms of auxiliary fields. Therefore, Eq. (26) is in fact fully anticipated.

### B. Electric dipole moment

The similar procedure can be applied to the electric system to obtain an electric dipole moment operator. The delta functional we insert into (12) is

$$\delta[E^z - \epsilon^{12jk}\partial_j a_k(x)]$$
$$\sim \int \mathcal{D}b_z \exp\left[i\int d^4x\, b_z(x)(E_z - \epsilon^{12jk}\partial_j a_k(x))\right], \quad (27)$$

where $j$, $k = 0, 3$, and $E^z$ is taken to be the Euclidean quantum field including the instanton configurations (10) and quantum fluctuations around them.

We follow the same procedure as before by integrating out the auxiliary field $b_z(x)$. It leads to the following Euclidean Lagrangian density analogous to Eq. (23) describing the magnetic case:

$$\mathcal{L} = -\frac{1}{2}(\epsilon^{12jk}\partial_j a_k(x))^2 + \frac{2\pi k + \theta_{\text{eff}}^E}{e\beta L_3}(\epsilon^{12jk}\partial_j a_k(x)). \quad (28)$$

All the comments after Eq. (23) also apply here for the electric case (28). Furthermore, there is an additional complication for the electric case due to the necessity for a transition to physical Minskowski space-time; i.e., we have to replace the Euclidean $\theta_{\text{eff}}^E$ in (28) by the Minkowski expression $\theta_{\text{eff}}^E$ according to relation (14),

$$\mathcal{L} = -\frac{1}{2}(\epsilon^{12jk}\partial_j a_k(x))^2 + \frac{2\pi k + i\theta_{\text{eff}}^M}{e\beta L_3}(\epsilon^{12jk}\partial_j a_k(x)), \quad (29)$$

where $\theta_{\text{eff}}^M = e\beta L_3 E_{\text{ext}}^{\text{Mink}}$ represents the physical electric field. The only difference from the magnetic case is the emergence of the factor $i$ in front of the effective theta parameter. Thus, we identify the electric dipole moment operator in Minkowski space-time with $[-i\epsilon^{12jk}\partial_j a_k(x)]V$. In what follows, we confirm this conjecture by explicit computation of the corresponding expectation value.

To proceed with this task, we make a shift,

$$\epsilon^{12jk}\partial_j a_k'(x) = \epsilon^{12jk}\partial_j a_k(x) - \frac{2\pi k + i\theta_{\text{eff}}^M}{eL_3\beta}, \quad (30)$$

such that the Lagrangian (29) in terms of the new variable $a_k'(x)$ becomes

$$\mathcal{L} = -\frac{1}{2}(\epsilon^{12jk}\partial_j a_k'(x))^2 + \frac{1}{2}\left(\frac{2\pi k + i\theta_{\text{eff}}^M}{eL_3\beta}\right)^2. \quad (31)$$

We can now calculate the expectation value of the electric dipole moment,

$$\langle p_{\text{ind}}^{\text{Mink}}\rangle = \langle[-i\epsilon^{12jk}\partial_j a_k(x)]\rangle V$$
$$= \frac{\sum_{k\in\mathbb{Z}}\int \mathcal{D}a\, e^{-\int d^4x\mathcal{L}}(-i\epsilon^{12jk}\partial_j a_k'(x) - i\frac{2\pi k}{eL_3\beta})V}{\sum_{k\in\mathbb{Z}}\int \mathcal{D}a\, e^{-\int d^4x\mathcal{L}}}$$
$$= \frac{\sum_{k\in\mathbb{Z}}(-i\frac{2\pi L_1 L_2 k}{e\beta})\exp[-\eta(\pi^2 k^2 + i\pi k\theta_{\text{eff}}^M)]}{\sum_{k\in\mathbb{Z}}\exp[-\eta(\pi^2 k^2 + i\pi k\theta_{\text{eff}}^M)]}$$
$$= -\frac{1}{\bar{\mathcal{Z}}_{\text{top}}}\sum_{k\in\mathbb{Z}}\frac{2\pi k L_1 L_2}{e\beta}e^{-\eta\pi^2 k^2}\sin(\pi k\eta\theta_{\text{eff}}^M), \quad (32)$$

where $\bar{\mathcal{Z}}_{\text{top}}$ is defined in (13). Here, we have removed the constant external term to keep only the truly induced contribution to the dipole moment, consistent with our previous definition in Sec. II B. Equation (32) exactly reproduces our previous expression (17) which was originally derived without even mentioning any auxiliary fields. This supports once again our formal manipulations with the auxiliary fields, and it also confirms our interpretation of the operator $[-i\epsilon^{12jk}\partial_j a_k(x)]$ as the quantum polarization operator of the system. All the comments we have made in Sec. III A regarding the physical meaning of this operator also apply here to the electric case, including the connection with Berry's phase, which we will not repeat here.

To study the quantum mechanical dipole transitions, we must work in Minkowski space-time where the metric signature allows for propagating on-shell photons. Although the original derivation in this section is performed in Euclidean space-time, we claim that the dipole moment operator $P_z \equiv [-i\epsilon^{12jk}\partial_j a_k(x)]V$ represents an operator in Minkowski space-time, as confirmed by the explicit expectation value calculation (32).

Our next task is to infer from our previous Euclidean path integral computations the structure of the quantum states, which can then be employed for conventional quantum dipole transitions in Minkowski terms; see footnote 1 and the related paragraph for an explanation of the source of this technical subtlety.

## IV. METASTABLE QUANTUM STATES IN THE MAXWELL SYSTEM

The main goal of this section is to identify quantum mechanical states in Hilbert space in Minkowski space using the operators constructed in the previous section, Sec. III. These quantum states have never been explicitly

---

[5]These similarities, in particular, include the following features: while $a_i(\mathbf{k})$ and $\mathcal{A}_i(\mathbf{k})$ are gauge-dependent objects, the observables, such as polarization or magnetization (26), are gauge invariant (modulo $2\pi$) characteristics. Furthermore, the main features of the systems in both cases are formulated in terms of global rather than local characteristics.

constructed in the previous path integral treatment of this model [1–5]. We substantiate our identification by reproducing the computed transition matrix elements with corresponding path integral computations in Euclidean space.

Before we proceed, we would like to give an overview of a well-known formal mathematical analogy between the construction of the $|\theta\rangle$-vacuum states in gauge theories and Bloch's construction of the allowed/forbidden bands in CM physics (see, e.g., Ref. [20]). The large gauge transformation operator $\mathcal{T}$ plays the role of the crystal translation operator in CM physics. $\mathcal{T}$ commutes with the Hamiltonian $H$ and changes the topological sector of the system

$$\mathcal{T}|m\rangle = |m + 1\rangle, \qquad [H, \mathcal{T}] = 0, \qquad (33)$$

such that the $|\theta\rangle$-vacuum state is an eigenstate of the large gauge transformation operator $\mathcal{T}$:

$$|\theta\rangle = \sum_{m\in\mathbb{Z}} e^{im\theta}|m\rangle, \qquad \mathcal{T}|\theta\rangle = e^{-i\theta}|\theta\rangle.$$

The $\theta$ parameter in this construction plays the role of the "quasimomentum" $\theta \to qa$ of a quasiparticle propagating in the allowed energy band in a crystal lattice with unit cell length $a$.

An important element, which is typically skipped in presenting this analogy but plays a key role in our studies, is the presence of the Brillouin zones classified by integers $k$. Complete classification can be either presented in the so-called extended zone scheme where $-\infty < qa < +\infty$ or the reduced zone scheme where each state is classified by two numbers, the quasimomentum $-\pi \leq qa \leq +\pi$ and the Brillouin zone number $k$.

In the classification of the vacuum states, this corresponds to describing the system by two numbers $|\theta, k\rangle$, where $\theta$ is assumed to be varied in the conventional range $\theta \in [0, 2\pi)$, while the integer $k$ describes the ground state (for $k = 0$) or the excited metastable vacuum states ($k \neq 0$). In most studies devoted to the analysis of the $\theta$ vacua, the questions related to the metastable vacuum states have not been addressed. Nevertheless, it has been known for some time that the metastable vacuum states must be present in non-Abelian gauge systems in the large $N$ limit [21]. A similar conclusion also follows from the holographic description of QCD as originally discussed in Ref. [22]. Furthermore, the metastable vacuum states can be explicitly constructed in a weakly coupled "deformed QCD" model [23].

Such metastable states will also emerge in our Maxwell systems defined on a compact manifold. Thus, the complete classification of the states in our system is $|\theta_{\text{eff}}, k\rangle$, where the integer $k$ plays a role similar to the $k$th Brillouin zone in the reduced zone classification as we discussed above.

## A. Identification of quantum states: Magnetic system

Through the formal manipulation in Sec. III A, we have identified the magnetic dipole moment operator $M_z = -\epsilon^{zjk}\partial_j a_k(x) \cdot V$. We have also seen that the quantum mechanical expectation value of $\langle M_z \rangle$ reproduces the expectation value $\langle m_{\text{ind}}^{\text{Mink}} \rangle$ computed using Euclidean path integrals (8), i.e.,

$$\langle M_z \rangle = -\left(\frac{2\pi L_3}{e}\right) \frac{\sum_{k\in\mathbb{Z}} k \exp[-\tau\pi^2(k + \frac{\theta_{\text{eff}}}{2\pi})^2]}{\sum_{k\in\mathbb{Z}} \exp[-\tau\pi^2(k + \frac{\theta_{\text{eff}}}{2\pi})^2]}. \quad (34)$$

Formula (34) determines a truly induced magnetic moment when the trivial constant contribution (related to the external magnetic field) is removed from the corresponding expression (8). Formula (34) was derived using conventional path integrals in Euclidean space-time without interpreting it in terms of any physical states.

Now, we interpret the result (34) in terms of quantum mechanical states in Hilbert space. First, the factor $\exp[-\tau\pi^2 k^2]$ originates from the partition function $\mathcal{Z}_{\text{top}}(\tau, \theta_{\text{eff}})$ (4). This exponential form in Euclidean space suggests that the combination

$$\epsilon(k) = \frac{\tau\pi^2 k^2}{\beta} = \frac{2L_3\pi^2 k^2}{e^2 L_1 L_2} \quad (35)$$

can be interpreted as the energy of state $|k\rangle$ for $\theta_{\text{eff}} = 0$ in Minkowski space. In the case of a nonzero external field $\theta_{\text{eff}} \neq 0$, the corresponding energy levels get shifted accordingly as in the well-known problem for a particle on a circle,

$$\epsilon(k, \theta_{\text{eff}}) = \frac{\tau\pi^2(k + \frac{\theta_{\text{eff}}}{2\pi})^2}{\beta}. \quad (36)$$

We identify the parameter $k$ with the label of the metastable vacuum state $|k\rangle$, similar to the classification of the $k$th Brillouin zone in CM systems mentioned above. This interpretation is supported by the observation that for $k = 0$ the energy $\epsilon(k = 0, \theta_{\text{eff}}) = \frac{1}{2}(VB_{\text{ext}}^2)$ is precisely the magnetic energy of the external field, while quantum tunneling generates the excited $|\theta_{\text{eff}}, k\rangle$ states with energies (36). In contrast to conventional quantum states in the context of dipole transitions, the "states" in our system are the $k$-instantons that describe tunneling transitions between the infinitely many degenerate vacuum winding states.

Once we accept this interpretation along with the identification of the magnetic dipole moment operator $M_z = -\epsilon^{zjk}\partial_j a_k(x) \cdot V$, we then proceed to interpret the corresponding factor in (34) as the nonvanishing transition matrix element $\langle k|M_z|0\rangle$ rather than a diagonal expectation value $\langle k|M_z|k\rangle$.

To simplify notations in what follows, we consider vanishing external field $\theta_{\text{eff}} = 0$ and the lowest excited

metastable state $k = 1$, which can be formally achieved by considering the limit $\tau \gg 1$. In this case, we can interpret (34) as the transition matrix element between the first excited state and the ground state,

$$\langle k = 0 | M_z | k = 1 \rangle \simeq -\frac{2\pi L_3}{e} \cdot e^{-\tau \pi^2}. \qquad (37)$$

The main argument behind this interpretation is the observation that the integer parameter $k$ which enters (34) originally appeared in the Euclidean path integrals as the instanton action describing the *interpolation* between two topologically distinct states according to Eq. (4). The same interpretation also follows from the boundary conditions (1) such that (37) can be thought of (in Minkowski terminology) as the configuration describing the transition matrix element between the states which satisfy the nontrivial boundary conditions (1) with $k = 1$ and states which satisfy the trivial boundary conditions with $k = 0$.

Yet another argument supporting the Hamiltonian interpretation in terms of the transition matrix elements (37) is the successful matching of our final formula for the intensity of radiation with the classical expression for emission (20) discussed in Sec. II C. Indeed, the conventional quantum mechanical formula for the probability for the quantum transition per unit time is known to match well with the classical formula (20) for the intensity of radiation. This spectacular example of classical correspondence implies that the probability for the quantum emission $R_{1\to0}$ is expressed in terms of the transition matrix element (37) to match the classical formula (20),

$$R_{1\to0} = \frac{\omega^3 \mu_0}{3\pi \hbar c^3} |\langle k = 0 | M_z | k = 1 \rangle|^2, \qquad \hbar\omega R_{1\to0} \to \langle I^M \rangle. \qquad (38)$$

In this well-known correspondence, the magnetic moment $m_{ind}$ as usual is identified with the time-dependent transition matrix element $m_{ind}(t) = [\langle k = 0 | M_z | k = 1 \rangle e^{-i\omega t}]$. In this case, the magnetic moment entering formula (20) for the classical emission should be identified with $[m_{ind}(t) + m_{ind}^*(t)] \sim 2\cos(\omega t)$, while the magnetic moment entering the quantum mechanical expression (38) should be identified with the transition matrix element (37). This well-known correspondence between classical and quantum descriptions once again supports our interpretation of (37) as the transition matrix element between the excited and ground states, though the original computations (34) from which formula (37) was inferred were performed in the Euclidean path integral approach without any notions of the Hamiltonian formulation.

We conclude with the following remarks. As we mentioned previously, the expectation value (34) vanishes when the external field is zero, though we claim that the transition matrix element (which eventually leads to the emission of

real photons) does not vanish according to (37). There is no contradiction here as the expectation value (34) vanishes at $\theta_{eff} = 0$ as a result of cancellation between $k = \pm 1$ states, while in our discussions above, we selected a single state $|k = 1\rangle$ which obviously must be somehow produced by nonequilibrium dynamics and separated from the $|k = -1\rangle$ state.

Finally, the transitions between the quantum states $|k = 1\rangle \to |k = 0\rangle$ described here should not be confused with multiple tunneling transitions between the infinitely degenerate $|n\rangle$ vacuum winding states that make up the $\theta$-vacuum, classified by two parameters $|\theta_{eff}, k\rangle$ as discussed at the very beginning of this section. Unlike the vacuum winding states, these quantum states are separated in energy (35), and the transitions between them form the central subject of this section.

## B. Identification of quantum states: Electric system

Through the formal manipulation in Sec. III B, we have identified the dipole moment operator $P_z = -i\epsilon^{12jk}\partial_j a_k(x) \cdot V$, the quantum mechanical expectation value of which reproduces the expectation value $\langle p_{ind}^{Mink} \rangle$ computed in the Euclidean path integral approach, i.e.,

$$\langle P_z \rangle = -\frac{1}{\mathcal{Z}_{top}} \sum_{k\in\mathbb{Z}} \frac{2\pi k L_1 L_2}{e\beta} e^{-\eta\pi^2 k^2} \sin(\pi k\eta\theta_{eff}^M). \qquad (39)$$

Following the magnetic system in the previous section, we wish to interpret this expression in terms of quantum states in Hilbert space. In the $\theta_{eff}^M = 0$ limit, the energy of each state can be read off the Boltzmann factors,

$$\epsilon(k) = \frac{\eta\pi^2 k^2}{\beta} = \frac{2\pi^2 k^2 L_1 L_2}{e^2 \beta^2 L_3}, \qquad (40)$$

analogous to (35). As in Sec. IV A, we work in the reduced zone scheme with $\theta_{eff}^M \in [-\pi, \pi]$ and identify the configurations labeled by integers $k$ as the quantum states $|k\rangle$. In particular, $k = 0$ is the ground state, and $k \neq 0$ represents the excited metastable states. The supporting arguments made in Sec. IV A apply to the electric system as well.

This connection allows us to further identify the transition elements of the $P_z$ matrix from (39) where we keep only the $k = 1$ state to simplify the notations,

$$\langle k = 0 | P_z | k = 1 \rangle = -i \frac{2\pi L_1 L_2}{e\beta} e^{-\eta(\pi^2 + i\pi\theta_{eff}^M)}, \qquad (41)$$

which is analogous to formula (37) for the magnetic system.

One can repeat the arguments presented in the previous subsection, Sec. IV A, to infer that the correspondence formula for the electric dipole transition assumes the form

$$R_{1\to 0} = \frac{\omega^3}{3\pi\hbar c^3 \epsilon_0}|\langle k=0|P_z|k=1\rangle|^2, \qquad \hbar\omega R_{1\to 0} \to \langle I^E\rangle.$$

$$(42)$$

This example of classical correspondence implies that the probability for the electric dipole transition $R_{1\to 0}$ is expressed in terms of the transition matrix element (41) to match the classical formula (20).

Our comments after Eq. (38) for the magnetic case still hold for the electric case, and we shall not repeat them here. The only additional remark we would like to make to conclude this section is as follows. All our results on the identification of the dipole moment operators and their expectation values (34) and (39) are based on the Euclidean path integral approach. We did not and could not construct the corresponding Hilbert space and the corresponding wave functionals $\Psi_k[A_i]$ in Minkowski space-time, which would depend on the E&M field configurations. However, using the correspondence principle (and some other hints and indications), we were able to reconstruct the relevant matrix elements (37) and (41) without complete knowledge of the wave functionals $\Psi_k[A_i]$. Fortunately, this is the only information we need in our following studies of quantum dipole transitions in a cavity.

## V. QUANTUM DIPOLE TRANSITIONS IN A CAVITY

The goal of this section is to construct the effective Lagrangian describing the interaction between the physical E&M fields and the auxiliary fields introduced in Secs. III and IV. This coupling will allow us to carry out proper quantum computations for the rate of emission of real physical photons, because the relevant transition matrix elements (37) and (41) have been computed in Minkowski space-time. This puts us in a position to use the well-developed procedure to study quantum dipole transitions, such as in the phenomenon of stimulated emission.

Numerically, the decay rate (42) is extremely low (see Sec. V C for numerical estimates). It has been known for quite some time that different types of microwave (optical) cavities can drastically increase the sensitivity for photon detection. Due to the smallness of the magnitude of all the topological effects of our Maxwell system, including the intensity of photon radiation, there might be hope that the stimulated emission of photons from the capacitor configuration can be detected using microwave (optical) resonators.

Essentially, we adopt the conventional technique normally used to study a system consisting of an atom in an optical cavity. The role of the atom in our case is played by the topological Maxwell system as described in the previous sections, while the optical cavity is replaced by a microwave cavity as the typical frequencies for our system are much smaller than atomic frequencies.

However, it should be noted that a specific design for microwave cavities in a possible experiment is certainly beyond the scope of this paper, and we shall proceed with only a general sketch of the possible experimental setup for illustrative purposes exclusively. Our numerical estimates given in Sec. V C suggest that the typical sizes where persistent currents have been observed and where coherent Aharonov-Bohm phases can be maintained could be a good starting point for a possible design. However, we are reluctant to put forward a specific experimental setup since our main goal is to describe a new phenomenon, rather than to design a device for its observation or measurement. We leave the questions on possible design for others in the community who can then use their own expertise to devise suitable experimental apparatuses.

### A. Coupling with quantum E&M field

First, we want to demonstrate that the quantum propagating E&M field couples to the magnetic and electric dipole moment operators $M_z$ and $P_z$ in exactly the same way as it does to the dipole moment operators in conventional quantum mechanics. Indeed, from (23), one can deduce that the interaction of the quantum field $B^{\text{quant}}$ with the auxiliary fields $a_k(x)$ is given by the following extra term $\Delta\mathcal{L}^M_{\text{int}}$ in the Lagrangian,

$$\Delta\mathcal{L}^M_{\text{int}} = B^{\text{quant}}_z \cdot [\epsilon^{zjk}\partial_j a_k(x)], \qquad (43)$$

where $\vec{B}^{\text{quant}} = \vec{\nabla} \times \vec{A}^{\text{quant}}$ is expressed in terms of the conventional quantum propagating field $\vec{A}^{\text{quant}}$. The relation (43) follows from the fact that the $\theta_{\text{eff}}$ parameter entering (23) represents the total E&M field, including the classical and the quantum parts, i.e., $\theta_{\text{eff}} = eL_1L_2(B^{\text{class}}_z + B^{\text{quant}}_z)$. In our previous discussions, we kept only the classical, constant, portion of the field. In our present discussions in this section, we obviously need the quantum, fluctuating, portion of the field as well.

The expression (43) obviously has the structure of a quantum field $B^{\text{quant}}$ interacting with the magnetic moment operator expressed in terms of the auxiliary fields and derived in (26) using the Euclidean path integral approach. Precisely, the matrix element of this operator has been computed in (37). The operator $M_z$ and its transition matrix element play the same role in our computations as the electron magnetic moment operator $\vec{\mu} = \frac{e\hbar}{2mc}(\vec{l} + 2\vec{s})$ and the corresponding matrix elements do in atomic physics with the conventional coupling $-\vec{\mu}\cdot\vec{B}$.

The same arguments also apply to the quantum coupling of the E&M quantum field with the electric dipole moment operator $P_z$. Indeed, from (29), one can deduce that the interaction of the quantum field $E^{\text{quant}}$ with the auxiliary field $a_k(x)$ is given by the following extra term $\Delta\mathcal{L}^E_{\text{int}}$ in the Lagrangian:

$$\Delta \mathcal{L}_{\text{int}}^{E} = E_{z}^{\text{quant}} \cdot [i\epsilon^{12jk}\partial_{j}a_{k}(x)]. \tag{44}$$

This is because $\theta_{\text{eff}}^{M}$ which enters (29) represents the physical electric field, including the constant external part and the fluctuating quantum part. The expression (44) obviously has the structure of the interaction between the quantum field $E^{\text{quant}}$ and an electric dipole operator expressed in terms of the auxiliary fields and derived in (32) using the Euclidean path integral approach. Precisely, the matrix element of this operator has been computed in the previous section (41). The operator $P_z$ and its transition matrix element play the same role as the electron dipole moment operator $\vec{d} = e\vec{r}$ and the corresponding matrix elements do in atomic physics with conventional coupling $-\vec{d} \cdot \vec{E}$.

The essence of the auxiliary fields $a_k(x)$ employed above is that they effectively account for the interaction between nontrivial topological configurations (which themselves describe the tunneling events) and the propagating physical photons. All the relevant information about these auxiliary fields, originally introduced in the Euclidean path integral approach, is encoded now in terms of the matrix elements (37) and (41) in Minkowski space-time such that one can proceed with the computations of the quantum transitions using conventional Hamiltonian techniques, which we shall do in the next section.

## B. Jaynes-Cummings Hamiltonian for the topological Maxwell system

We consider the electric system and limit ourselves to two states: an excited state $|k = 1\rangle$ and the ground state $|k = 0\rangle$. The two levels are separated by an energy difference $\hbar\omega_0 = \epsilon(1) - \epsilon(0) = \eta\pi^2/\beta$ according to (40). Here, we use the notation $|n, k\rangle \equiv |n\rangle \otimes |k\rangle$, where $n$ is the number of photons (not to be confused with $|m\rangle$ being the winding states) and $k \in \mathbb{Z}$ indicates the state of the $\mathcal{TV}$. Suppose we prepare the system in the $|k = 1\rangle$ state and tune the oscillating external field to the resonance frequency $\omega_0$. The transition rate from the $|k = 1\rangle$ to the $|k = 0\rangle$ state is determined by the corresponding transition matrix element (41) inferred previously from the Euclidean path integral computations (39).

First, as the energy of the $k$-states grow quadratically with $k$, $\epsilon(k) \sim k^2$, we can neglect highly excited metastable states by considering only the leading contributions to the dipole moment (41) due to the transition from $|k = 1\rangle$ to $|k = 0\rangle$. To simplify the analysis and to emphasize the basic features of the system, we also neglect the $|k = -1\rangle$ state which is degenerate to the $|k = 1\rangle$ state for vanishing external fields. In principle, it can be easily accounted for. However, we want to make our formulas as simple as possible, and we ignore this extra state for now.

If we assume that only a single cavity mode $\omega_0$ exists, which is a good approximation in the case of a high Q

resonator, the system can be described by the Jaynes-Cummings Hamiltonian,

$$H = H_0 + H_I$$
$$H_0 = \hbar\omega_0 a^{\dagger}a + \frac{\hbar\omega_a}{2}\sigma_z,$$
$$H_I = \hbar(ga\sigma_+ + g^* a^{\dagger}\sigma_-), \tag{45}$$

coupling a single harmonic oscillator degree of freedom to our two-level system $|k = 0\rangle$ and $|k = 1\rangle$. Here, $\sigma_{\pm} \equiv \frac{1}{2}(\sigma_x \pm i\sigma_y)$, and $g$ describes the coupling of our two-level system with the quantized E&M field with two transverse polarizations. Assuming the E&M field is polarized in the $z$-direction, $g$ reads

$$g = -i\sqrt{\frac{\omega}{2\hbar V}}\langle k = 0|P_z|k = 1\rangle. \tag{46}$$

One can easily check that on resonance, $\omega_0 = \omega_a$, the interaction Hamiltonian $H_I$ commutes with the free Hamiltonian $H_0$, i.e., $[H_0, H_I] = 0$. Therefore, the eigenstates of the full Hamiltonian $H$ can be written as a linear combination of the degenerate eigenstates of $H_0$. The degenerate eigenstates of $H_0$ are $|n, 1\rangle$ and $|n + 1, 0\rangle$. Within this degenerate subspace, the state of the system at time $t$ can be written $|\Psi(t)\rangle = c_{n,1}(t)|n, 1\rangle + c_{n+1,0}(t)|n+1, 0\rangle$, and the dressed eigenstates of the full Hamiltonian are $\frac{1}{\sqrt{2}}(|n, 1\rangle \pm |n + 1, 0\rangle)$. Solving the Schrödinger equation yields the time evolution

$$c_{n,1}(t) = c_{n,1}(0)\cos(\Omega_n t) - ic_{n+1,0}(0)\sin(\Omega_n t)$$
$$c_{n+1,0}(t) = c_{n+1,0}(0)\cos(\Omega_n t) - ic_{n,1}(0)\sin(\Omega_n t), \tag{47}$$

where $\Omega_n = |g|\sqrt{n + 1}$.

In particular, if we prepare the $\mathcal{TV}$ in its excited state $|k = 1\rangle$ and the initial cavity field with $n$ photons, i.e., $c_{n,1}(0) = 1$ and $c_{n+1,0}(0) = 0$, then at a later time $t$, the probability for finding the vacuum in the $|k = 1\rangle$ state is

$$P_{k=1} = |\langle n, 1|\Psi(t)\rangle|^2 = \frac{1}{2}(1 + \cos 2\Omega_n t). \tag{48}$$

The sinusoidal oscillation indicates that energy is constantly exchanged between the $\mathcal{TV}$ and the cavity field. This is, of course, the conventional Rabi oscillations with the only difference being that, instead of a two-level atomic system, the transitions in our case occur between the metastable and ground states in the $\mathcal{TV}$, similar to the Brillouin zone classification as discussed at the very beginning of Sec. IV.

It is particularly interesting to investigate the dynamics of our system ($\mathcal{TV}$ plus the quantum E&M field) when we start with an initial cavity field that is a coherent state of photons:

$$|\alpha\rangle = e^{-|\alpha|^2/2} \sum_n \frac{\alpha^n}{\sqrt{n!}} |n\rangle. \qquad (49)$$

The time evolution of the $|k = 1\rangle$ state probability is

$$P_{k=1} \approx \frac{1}{2} \left[ 1 + \sum_{n=0}^{\infty} \frac{e^{-|\alpha|^2} |\alpha|^{2n}}{n!} \cos(2\Omega_n t) \right]. \qquad (50)$$

We conclude this subsection with the following remark. The rate of emission from $\mathcal{TV}$ due to the nonstationary TCE is very low. Nevertheless, it is not hopeless to eventually measure this fundamentally new type of energy. The proposal presented in this section is to use resonant cavities for such measurements. A number of historical examples show that such a goal can in principle be achieved.[6]

### C. Numerical estimates

Here, we take the realistic experimental parameters used in Refs. [4,5] to estimate the dipole transition rates for the magnetic (38) and electric (42) systems as well as the lifetime of the excited states.

For the magnetic system, we use the sample parameters from the experiment on persistent currents [25]. The sample in this case was a metallic ring with area $L_1 \times L_2 = \pi(1.2~\mu m)^2$ and thickness $L_3 = 0.1~\mu m$ at a temperature of $\beta = 0.6$ cm. The observation of persistent currents implies that coherent Aharonov-Bohm (AB) phases, which are also crucial for the experimental realization of the TCE, can be maintained (see more elaboration on this point in Sec. VI A in Ref. [5]). Although it was demonstrated in Ref. [4] that for this particular setup $\tau \gg 1$ such that all topological effects are vanishingly small, we assume here that $\tau \sim 1$ can somehow be achieved. In this case, the energy separation between the ground ($k = 0$) and excited ($k = 1$) states is

$$\hbar\omega_a \approx 3.2 \times 10^{-4}~\text{eV}. \qquad (51)$$

The resonant wavelength corresponding to this energy is 3.8 mm, much larger than the dimensions of the system, thereby justifying the dipole approximation in (38). The transition rate from the excited to the ground state is then

$$R_{1\to0} \approx 1.6 \times 10^{-3}~\text{s}^{-1}, \qquad (52)$$

which corresponds to an excited state lifetime of $6 \times 10^2$ s.

For the electric system, we use the two sets of parameters in Ref. [5]. The first set of parameters is motivated by the accurate measurement of the CE using parallel plates [26] (see also Ref. [27] where historically the first accurate measurement was performed, but for a different geometry). The second set of parameters is motivated by the experiments on persistent currents [25] where the correlation of the AB phases is known to be maintained. While the persistent current is a magnetic phenomenon, electromagnetic duality strongly suggests that a similar electric effect should also occur when coherent AB phases are correlated over macroscopically large distances.[7] Therefore, for the second set of parameters, we adopt the typical sizes of the magnetic system used above (where persistent currents have been observed) to estimate the topological effects in the electric capacitor configuration. Both sets of parameters can optimize the TCE:

$$\eta^{(I)} = \frac{2L_1 L_2}{e^2 \beta L_3} = \frac{1.2 \times 1.2~\text{mm}^2}{2\pi\alpha(180~\text{mm})(0.4~\text{mm})} \approx 0.4, \qquad (53)$$

$$\eta^{(II)} = \frac{2L_1 L_2}{e^2 \beta L_3} = \frac{2\pi(1.2~\mu m)^2}{4\pi\alpha(0.6~\text{cm})(0.1~\mu m)} \approx 0.16. \qquad (54)$$

The energy separations between the ground ($k = 0$) and excited ($k = 1$) states are

$$\hbar\omega_a^{(I)} = 4.8 \times 10^{-6}~\text{eV}, \qquad \hbar\omega_a^{(II)} = 5.2 \times 10^{-5}~\text{eV}. \qquad (55)$$

For both sets of parameters, the electric dipole approximation in (42) can be justified by observing that the resonance external electric fields correspond to wavelengths that are much larger than the sizes of the respective systems:

$$\lambda^{(I)} \approx 0.3~\text{m} \qquad \lambda^{(II)} \approx 0.02~\text{m}. \qquad (56)$$

The induced dipole moments for our two sets of parameters can be estimated as [5]

$$\langle p_{\text{ind}}^{\text{Mink}}\rangle^{(I)} \approx \frac{eL_3}{2} \eta^{(I)} \sim 0.1~(e \cdot \text{mm})$$

$$\langle p_{\text{ind}}^{\text{Mink}}\rangle^{(II)} \approx \frac{eL_3}{2} \eta^{(II)} \sim 0.01~(e \cdot \mu m). \qquad (57)$$

These estimates suggest that the effective number of degrees of freedom $n_{\text{eff}}$ which coherently generate the

---

[6]One can mention a recent example of the measurement of spontaneous emission in silicon coupled to a superconducting microwave cavity. The relaxation rate is increased by 3 orders of magnitude as the spins are tuned to cavity resonance [24].

[7]An interesting impact of AB phases on tunneling rates has been recently demonstrated in Ref. [28], where photon emission occurs exactly during the tunneling events. The difference from our case is that the tunneling in our system occurs between distinct topological vacuum sectors $|m\rangle$, while in Ref. [28] the charged particle tunnels in the conventional quantum mechanical sense.

dipole moments (57) and the corresponding transitions (58) can be estimated as $\langle p_{\mathrm{ind}}^{\mathrm{Mink}}\rangle/(e\times 10^{-8}\ \mathrm{cm})$, which numerically correspond to $n_{\mathrm{eff}}^{(I)}\sim 10^{6}$ and $n_{\mathrm{eff}}^{(II)}\sim 10^{2}$.

The transition rates (42) for the two sets of parameters are

$$R_{1\to 0}^{(I)}\approx 0.21\ \mathrm{s}^{-1},\qquad R_{1\to 0}^{(II)}\approx 5.7\times 10^{-4}\ \mathrm{s}^{-1},\qquad (58)$$

so the lifetimes of the excited states are 4.7 and $1.7\times 10^{3}$ s respectively.

One should emphasize that, in contrast to conventional systems where a large number of spins are present in a sample, our sets of parameters (53) and (54) describe a small but single macroscopic quantum coherent system. Therefore, a potential detector must be sensitive to a single photon to observe this new effect of emission from the $\mathcal{TV}$.

The rates (58), of course, are highly sensitive to all dimensional parameters of the system and the temperature and show drastic changes when one puts a system into the background of an external field. In fact, this high sensitivity to the external field can be used to detect the topological vacuum effects as a conventional vacuum is largely unaffected by any external sources, as argued in Refs. [1,5]. Essentially, it means that one can scan the system by changing the external field to search for a resonance response. It also implies that one can, in principle, manipulate a system in very much the same way as one normally manipulates cold atom systems by tuning the external field.

## VI. CONCLUSION

Our conclusion can be separated into three related, but still distinct pieces:
  (i) Section VI A: solid theoretical results based on the Euclidean path integral computations in the Maxwell system defined on a compact manifold,
 (ii) Sec. VI B: relation to other approaches where real-time dynamics plays a key role
(iii) Sec. VI C: some speculations related to strongly coupled QCD realized in nature where fundamentally the same vacuum effects do occur and might be the crucial ingredients in understanding the observed cosmological vacuum energy. In fact, the Maxwell system which is the subject of the present work was originally invented as a theoretical toy model where some deep theoretical questions can be addressed (and answered) in a simplified setting.

### A. Basic results

In this work, we discussed a number of very unusual features exhibited by the Maxwell theory formulated on a compact manifold $\mathbb{M}$ with nontrivial topological mappings $\pi_{1}[U(1)]$, termed the topological vacuum ($\mathcal{TV}$). One of the properties which plays an important role in the present studies is the generation of metastable vacuum states, similar to the classification of Brillouin zones as discussed in Sec. IV. All these features originate from the topological portion of the partition function $\mathcal{Z}_{\mathrm{top}}$ which is a result of the tunneling events between physically identical but topologically distinct winding states $|n\rangle$. The relevant physics cannot be ascribed to physical propagating photons with two transverse polarizations. In other words, all effects discussed in this paper have a nondispersive nature.

The computations of the present work along with previous calculations of Refs. [1–5] imply that the extra energy (and entropy), not associated with any physical propagating degrees of freedom, may emerge in gauge systems if some conditions are met. This fundamentally new type of energy emerges as a result of the dynamics of pure gauge configurations and tunneling transitions between physically identical but topologically distinct winding states. The new idea advocated in this work is that this new type of energy can, in principle, be studied if one places the system in a time-dependent background, in which case we expect the topological vacuum configurations to radiate conventional propagating photons which can be detected and analyzed according to (38) and (42).

As we discussed in detail in the text, the fundamental technical obstacle for such an analysis is that the radiation of real physical particles on the mass shell is inherently formulated in Minkowski space-time with a well-defined Hilbert space of the asymptotic states. At the same time, the tunneling is described in terms of vacuum fluctuations (instanton fluxes) interpolating between the topological $|n\rangle$ winding sectors and is fundamentally formulated in Euclidian space-time; see footnote 1 for some comments on this problem. We overcame this technical obstacle by introducing auxiliary topological fields which, on the one hand, encode the entire information about the tunneling transitions and, on the other hand, can be analytically continued to Minkowski space-time. Eventually, this approach allowed us to turn the problem into conventional Hamiltonian dynamics formulated in Minkowski terms, as described in Secs. IV and V.

The corresponding rate of emission is very low for our system as estimated in Sec. V C. The hope is that microwave cavities may drastically enhance the emission rate such that radiated photons can be observed. Furthermore, putting the system in a background of external electric or magnetic fields, represented by $\theta_{\mathrm{eff}}$ in the paper, one can manipulate the system in pretty much the same way as one normally does with cold atom systems by tuning the external field. In practice, it means that one can scan the system by changing the external fields to search for a resonance response.

## B. Relation to other approaches

As emphasized above, we overcame the main technical obstacle in calculating the production of real particles (a real-time process in Minkowski space-time), while dealing with tunneling processes (formulated in Euclidean space-time) by introducing the auxiliary fields which can be easily continued to Minkowski space-time. This problem is obviously not unique to our work, but is, in fact, a common problem when path integrals are performed in Euclidean space-time while the relevant physical questions are formulated in Minkowski terms; see footnote 1.

There have been a number of different attempts to attack this problem. The most promising, in our view, is the approach based on formulating path integrals in Picard-Lefschetz theory. See recent reviews [29,30] and references to the original papers therein. The basic idea there is to formulate real-time path integrals. The field configurations which describe the tunneling processes live in a complexified field space. It turns out that the corresponding configurations, being singular, nevertheless produce a finite action for the path integral. In a few simple cases, the computations can be explicitly carried out to reproduce the known results in quantum mechanics (QM) systems (see original computations [31–33] and reviews [29,30]).

It is natural to expect that this approach, in principle, can be generalized to include a time-dependent background field, in which case the complex saddles should be able to describe tunneling transitions as well as particle production, precisely the topic of the present work. In other words, we strongly suspect that complex saddles which describe tunneling events in real-time path integrals may also contain information about the production of real particles in a time-dependent background. It remains to be seen how this information can be recovered from complex saddles. The answer to this question is not yet known, as recent studies [29,30] are mostly focused on analyzing the properties of the vacuum itself, rather than generalizing this approach to include a time-dependent background to study particle production rates.

## C. Speculations

The unique feature of the system where an extra energy is not related to any physical propagating degrees of freedom was the main motivation for the proposal [34–36] that the vacuum energy of the Universe may have, in fact, precisely such a nondispersive nature.[8] This proposal where an extra energy cannot be associated with any propagating particles should be contrasted with the conventional description where an extra vacuum energy in

the Universe is always associated with some *ad hoc* propagating degree of freedom.[9]

Essentially, the proposal [34–36] identifies the observed vacuum energy with the topological Casimir-type energy, which, however, does not originate from the dynamics of the physical propagating degrees of freedom but rather from the dynamics of the topological sectors that are always present in gauge systems and which are highly sensitive to arbitrary large distances. An explicit manifestation of this nondispersive nature of the vacuum energy in the model considered in the present work is the wrong sign of the kinetic term in the effective Lagrangians describing the dynamics of the auxiliary nonpropagating fields (23), (31). This wrong sign has exactly the same nature as the conjectured Veneziano ghost introduced in QCD to resolve the so-called $U(1)$ problem; see footnote 4 for a few comments on this matter. Furthermore, the radiation from the vacuum in a time-dependent background (which is the main subject of this work) is very similar in all respects to the radiation which might be responsible for the end of inflation in that proposal. The cosmological ideas of the proposal [34–36] can hopefully be tested in a tabletop experiment (which is the subject of the present paper) where the vacuum energy in a time-dependent background can be transferred to real propagating degrees of freedom as described in Sec. V. In cosmology, the corresponding period plays a crucial role and calls the reheating epoch which follows inflation with the vacuum energy being the dominant component of the Universe.

To conclude, the main point of the present studies is the claim that the emission of real photons may occur as a result of tunneling transitions between topologically distinct but physically identical winding $|n\rangle$ sectors, rather than from conventional physical propagating degrees of freedom.

## ACKNOWLEDGMENTS

---

[8]This new type of vacuum energy which cannot be expressed in terms of propagating degrees of freedom has in fact been well studied in QCD lattice simulations; see Ref. [34] with a large number of references on the original lattice results.

[9]There are two instances in the evolution of the Universe when the vacuum energy plays a crucial role. The first instance is identified with the inflationary epoch when the Hubble constant $H$ was almost constant, which corresponds to the de Sitter-type behavior $a(t) \sim \exp(Ht)$ with exponential growth of the size $a(t)$ of the Universe. The second instance where the vacuum energy plays a dominant role corresponds to the present epoch when the vacuum energy is identified with the so-called dark energy $\rho_{DE}$ which constitutes almost 70% of the critical density. In the proposal [34–36], the vacuum energy density can be estimated as $\rho_{DE} \sim H\Lambda_{QCD}^3 \sim (10^{-4} \text{ eV})^4$, which is amazingly close to the observed value.

## APPENDIX A: REVIEW OF THE INSTANTON SOLUTIONS

In this Appendix, we show how the instanton solutions (1) and (9) are derived. To do so, we first show how they are obtained in the original 2D Maxwell theory (i.e., Schwinger model without fermions) on a toroidal manifold and then extend the results to 4D.

### 1. 2D Maxwell theory

We follow Ref. [1] and references therein and solve the 2D Maxwell theory using both the physically transparent Hamiltonian approach and the Euclidean-space path integrals with instantons. Their exact agreement validates the use of instantons in this theory.

In the Hamiltonian approach, we define the system on a spatial circle of circumference $L$ at inverse temperature $\beta$.

We follow the procedure outlined in Refs. [1,37] to canonically quantize the 2D Maxwell system. First, we fix the gauge:

$$A_0 = 0 \qquad \partial_1 A_1 = 0. \tag{A1}$$

Hence, $A_0$ is not a dynamical variable. On the other hand, $E = \dot{A}_1(t)$. We impose conventional periodic boundary conditions:

$$A_1\left(t, x = -\frac{L}{2}\right) = A_1\left(t, x = \frac{L}{2}\right). \tag{A2}$$

The theory is defined by the following Hamiltonian density and commutation relations:

$$\mathcal{H} = \frac{1}{2}E^2 \tag{A3}$$

$$[A_1(x), E(y)] = i\delta(x - y). \tag{A4}$$

We also need to impose Gauss's law on the set of physical states $|\text{phys}\rangle$,

$$\partial_1 E|\text{phys}\rangle = 0, \tag{A5}$$

which is only satisfied by the $x$-independent zero mode. As it is known, there is a class of admissible gauge transformations, the so-called large gauge transformations

$$A_1 \to A_1 + \frac{d\alpha(x)}{dx}, \quad \alpha = \frac{2\pi n x}{eL}, \quad n = \pm 1, \pm 2.... \tag{A6}$$

This gauge function is compatible with periodic boundary conditions (A2) because $d\alpha(x)/dx = \text{const}$, and the periodicity (A2) is not violated. This implies the following gauge equivalence relation:

$$A_1 \sim A_1 + \frac{2\pi}{eL}n. \tag{A7}$$

Hence, we conclude that $A_1$ is not independent on the entire interval $(-\infty, \infty)$ and instead lives on a circle of circumference $2\pi/eL$.

By expanding $A_1$ and $E$ in their Fourier modes, we can map the current problem onto the particle on a ring problem in quantum mechanics. The conjugate momentum operator and the Hamiltonian read

$$E = -\frac{i}{L}\frac{d}{dA}, \tag{A8}$$

$$H = \frac{L}{2}\left(-\frac{i}{L}\frac{d}{dA}\right)^2. \tag{A9}$$

$H$ acting on the energy eigenstates $\exp(ienLA)$ yields the eigenvalues $\epsilon_n = \frac{1}{2}n^2 e^2 L$. The partition function at inverse temperature $\beta$ is therefore given by the canonical ensemble

$$\mathcal{Z} = \text{tr}e^{-\beta H} = \sum_n e^{-\beta \epsilon_n} = \sum_n \exp\left(-\frac{\beta e^2 L}{2}n^2\right), \tag{A10}$$

where we have taken the fundamental theta term, $\theta = 0$, to simply formulas and notations.

In the path integral approach (Refs. [1,12,13]), we solve the same problem in Euclidean space-time with metric (1,1). Time and space form a 2-torus with size $\beta \times L$. In the context of this problem, the topology of the system is equivalently taken into account by imposing periodic boundary conditions up to a large gauge transformation and using the so-called instanton solutions.

The Maxwell equations with the appropriate boundary conditions, for instance,

$$A_\mu(x_0, x_1 + L) = A_\mu(x_0, x_1) + \partial_\mu \frac{2\pi k}{\beta}x_0, \tag{A11}$$

yield solutions of the form

$$A_\mu^{(k)} = A_\mu^{(0)} + C_\mu^{(k)}, \tag{A12}$$

where $A_\mu^{(0)}$ is the exactly periodic quantum field and $C_\mu^{(k)}$ is the classical instanton solution.

In Lorenz gauge, the instanton solution can be written

$$A_\mu^{\text{top}} = C_\mu^{(k)} = \left(-\frac{\pi k}{eV}x_1, \frac{\pi k}{eV}x_0\right), \tag{A13}$$

where $V = \beta L$ is the volume of the Euclidean space-time. These instanton configurations classified by integers $k$ describe tunneling between different vacuum winding states, say $|m\rangle$ and $|m'\rangle$ with $k = m' - m$ [cf. Eq. (33)]. They also give rise to a topological electric field,

$$E_{\text{top}} = \partial_0 A_1^{\text{top}} - \partial_1 A_0^{\text{top}} = \frac{2\pi k}{eV}. \qquad (A14)$$

It is worth mentioning that the topological electric field (A14) should not be confused with the familiar physical electric field in Minkowski space-time, which is the eigenvalue of the $E$ operator (A8). Rather, it is an effective electric field in the unphysical Euclidean space-time and is better thought of as some complex configuration that saturates the Euclidean path integral and that describes tunneling transitions between distinct topological sectors. In particular, the dependence of these fields on the coupling constant $e$ is drastically different: the topological $E_{\text{top}}$ configuration describing the tunneling amplitude is proportional to $e^{-1}$, while the physical electric field being the eigenvalue of (A8) is proportional to $e$.

The partition function can be obtained by doing the following path integral and explicitly summing over topologies:

$$\mathcal{Z} = \sum_{k \in \mathbb{Z}} \int \mathcal{D}A_\mu^{(k)} e^{\int d^2 x(-\frac{1}{2}E^2)}. \qquad (A15)$$

Here, $E$ includes both the quantum fluctuations and the topological field (A14).

Omitting the computational details, the partition function is

$$\mathcal{Z} = \mathcal{Z}_{\text{quant}} \times \mathcal{Z}_{\text{top}} = \sqrt{\frac{2\pi}{e^2 V}} \sum_{k \in \mathbb{Z}} e^{-\frac{2\pi^2 k^2}{e^2 V}}. \qquad (A16)$$

Although this partition function (A16) looks different from the one obtained earlier in the Hamiltonian approach (A10), they are in fact dual expressions of each other related by the Poisson summation formula. Thus, although it is not straightforward how one can directly relate the boundary conditions in the Hamiltonian approach (A2) (i.e., strictly periodic) to those in the path integral approach (A11) (i.e., periodic up to a large gauge transformation, giving rise to the instantons), their agreement in the end validates the use of instantons. In fact, the relation between these two approaches is quite complicated; see detailed analysis in Ref. [13] and also related discussions in Ref. [19].

Our computational framework in the main body of this paper is entirely based on Euclidean path integrals. Therefore, in this framework, we impose the boundary conditions up to large gauge transformations, similar to the above discussions. The corresponding fields, such as (A14), should be interpreted as the field configurations (describing the tunneling processes between the topological sectors) saturating the path integral, not to be confused with real fields representing the eigenvalues of the system, as we already mentioned after Eq. (A14).

### a. 4D Maxwell theory

If we consider the Maxwell theory in 4D space-time, the topologies of the space-time become substantially more complicated. The same periodic boundary conditions up to a gauge potentially yields six different instanton solutions, corresponding to the six hypersurfaces in 4D. However, if require two of the dimensions of space-time to be much greater than the other two, we essentially dimensionally reduce the problem to the previous 2D problem. Again, there are six ways this can be done, and the electric and magnetic cases discussed in Secs. II A and II B are precisely two of them:

*Case 1*: $\beta, L_3 \ll L_1, L_2$.—The dominant instanton and the corresponding boundary conditions are a straightforward generalization of (A11), (A13):

$$A_{\text{top}}^\mu = \left(0, -\frac{\pi k}{eL_1 L_2} x_2, \frac{\pi k}{eL_1 L_2} x_1, 0\right). \qquad (A17)$$

This instanton configuration gives rise to a uniform "topological magnetic field" in the $z$-direction:

$$\vec{B}_{\text{top}} = \vec{\nabla} \times \vec{A}_{\text{top}} = \left(0, 0, \frac{2\pi k}{eL_1 L_2}\right),$$

$$\Phi = e \int dx_1 dx_2 B_{\text{top}}^z = 2\pi k. \qquad (A18)$$

*Case 2*: $\beta, L_3 \gg L_1, L_2$.—The instanton that contributes the most will be

$$A_{\text{top}}^3(\beta) = A_{\text{top}}^3(0) + \frac{2\pi k}{eL_3},$$

$$A_{\text{top}}^\mu(t) = \left(0, 0, 0, \frac{2\pi k}{eL_3 \beta} t\right), \qquad (A19)$$

which produces a uniform "topological electric field" in the $z$-direction:

$$\vec{E}_{\text{top}} = \dot{\vec{A}}_{\text{top}} = \left(0, 0, \frac{2\pi k}{eL_3 \beta}\right),$$

$$\Phi = e \int dt dx_3 E_{\text{top}}^z = 2\pi k. \qquad (A20)$$

Certainly, the instanton solution given in (A19) still exists in a system with the first set of dimensional reduction conditions $\beta, L_3 \ll L_1, L_2$, but the resulting action $S_2 \sim \int d^4 x (1/\beta L_3)^2$ will be much larger than that of the first type of instanton, $S_1 \sim \int d^4 x (1/L_1 L_2)^2$.

As in the 2D case, it is far from obvious how one can formulate the boundary conditions in real 4D Minkowski space-time as in the Hamiltonian approach and then explicitly derive the above boundary conditions for the Euclidean instantons. These instantons should be treated as

auxiliary field configurations saturating the path integral, and such an interpretation is further supported by our studies in the present work where the configurations saturating the path integral are in fact complex-valued fields, which obviously cannot be confused with real physical configurations. However, the exact analogy between the 2D and 4D cases achieved via dimensional reduction[10] strongly suggests that, similarly to the simple boundary conditions in the 2D Hamiltonian method (A2), all we need for real experiments in 4D Minkowski space-time is periodic boundary conditions in the relevant directions (without large gauge transformations).

In short, we require periodicity up to large gauge transformations to perform mathematical derivations in Euclidean space-time, whereas simple periodic boundary conditions are needed in Minkowksi space-time, both for Hamiltonian solutions and for experiments.

It is quite possible that formulating the path integral in Picard-Lefschetz theory using Minkowski space-time from the start, as mentioned in Sec. VI B, may give a precise answer to the relation between these two descriptions. However, the corresponding computational framework is not presently known and is yet to be developed.

# APPENDIX B: ON POSSIBLE DESIGN OF THE QUANTUM LC CIRCUITS IN REAL MINKOWSKI SPACE-TIME

We make a few comments here on the possible design of a system satisfying the periodic boundary conditions that represent the key element for generating $\mathcal{Z}_{\text{top}}$ from non-trivial $\pi_1[U(1)]$. As we emphasized in Appendix A, the construction in Minkowski space-time requires simple periodic boundary conditions. It is only our mathematical construction of the Euclidean path integral that requires more complicated boundary conditions (periodic up to large gauge transformations), which produce gauge images of the original interval where the gauge field is defined. In the path integral approach, the summation of an infinite number of gauge images is harmless as any expectation value is always computed by normalizing to the same partition function which also includes the same infinite sum.

The subject of the present Appendix is a possible design in Minkowski space-time. Therefore, we do not discuss Euclidean instantons nor configurations that saturate the Euclidean path integral. Instead, we focus on the physics in Minkowski space with exactly periodic boundary conditions (A2) and without summation over the gauge images. Experience with the 2D model reviewed in Appendix A shows that in Minkowski space-time such boundary

conditions do generate the topological physics studied in the present work.

*Case 1*: The simplest way to realize the periodic boundary conditions in magnetic systems is to make a cylinder as discussed in great detail in Ref. [4]. One can explicitly see that the fluctuating magnetic fluxes can be formulated in terms of boundary currents flowing along the cylinder. In many respects, the physics is very similar to (but still distinct from—see Ref. [4] for details) the persistent currents observed in a number of materials including metals, insulators, and semiconductors. In particular, the corresponding instanton fluxes would fluctuate even without an external magnetic field, in contrast to conventional persistent currents which occur exclusively due to the external magnetic field. The key requirement is, of course, that Aharonov-Bohm coherence be maintained in the entire system.

*Case 2*: The electric systems can be realized with a small capacitor consisting of two parallel plates with plate area $L_1 \times L_2$ and separation $L_3$, such as the mentioned in Secs. II B and V C. We connect the two plates with a superconducting wire. In the wire, the electromagnetic fields vanish, and the gauge fields $A_\mu$ must be a constant or its gauge transform. Therefore, the wire essentially identifies the two plates and enforces $A_\mu$ to be the same on the plates, giving conventional boundary conditions similar to (A2):

$$A_\mu(t, z = 0) = A_\mu(t, z = L_3). \quad (\text{B1})$$

The large gauge transformations along $z$,

$$A_3 \rightarrow A_3 + \frac{d\alpha(z)}{dz}, \qquad \psi \rightarrow e^{i\alpha(z)}\psi$$

$$\alpha = \frac{2\pi nz}{eL_3}, \qquad n = \pm 1, \pm 2...,$$

obviously respect the boundary conditions (B1) because $d\alpha(z)/dz = \text{const}$. Similarly to the 2D analysis, we conclude that the $A_3$ field lives on a circle of circumference $2\pi/eL_3$. Thus, the 2D system represents a dimensionally reduced version of the current 4D electric system, as the topological portion of the partition function for the 4D electric case (13) reduces exactly to the 2D partition function (A16) in the limit $L_1, L_2 \rightarrow 0$ accompanied by a proper rescaling of the coupling constant $e$. Hence, the similar $\mathbb{S}^1$ topological physics will be generated in the 4D system, which gives rise to the physically observable phenomena discussed in this paper.

---

[10]For example, we explicitly see that the topological portion of the partition function for the 4D electric case (13) reduces to the 2D partition function (A16) in the limit $L_1, L_2 \rightarrow 0$ accompanied by a proper rescaling of the coupling constant $e$.

[1] C. Cao, M. van Caspel, and A. R. Zhitnitsky, Phys. Rev. D **87**, 105012 (2013).
[2] A. R. Zhitnitsky, Phys. Rev. D **88**, 105029 (2013).
[3] A. Zhitnitsky, Phys. Rev. D **90**, 105007 (2014).
[4] A. R. Zhitnitsky, Phys. Rev. D **91**, 105027 (2015).
[5] C. Cao, Y. Yao, and A. R. Zhitnitsky, Phys. Rev. D **93**, 065049 (2016).
[6] H. B. G. Casimir, Kon. Ned. Akad. Wetensch. Proc. **51**, 793 (1948).
[7] G. Y. Cho and J. E. Moore, Ann. Phys. (Amsterdam) **326**, 1515 (2011).
[8] X.-G. Wen, ISRN Cond. Matt. Phys. **2013**, 198710 (2013).
[9] S. Sachdev, arXiv:1203.4565.
[10] A. Cortijo, F. Guinea, and M. A. H. Vozmediano, J. Phys. A **45**, 383001 (2012).
[11] G. E. Volovik, Lect. Notes Phys. **870**, 343 (2013).
[12] I. Sachs and A. Wipf, Helv. Phys. Acta **65**, 652 (1992); Ann. Phys. (N.Y.) **249**, 380 (1996); S. Azakov, H. Joos, and A. Wipf, Phys. Lett. B **479**, 245 (2000).
[13] S. Azakov, Int. J. Mod. Phys. A **21**, 6593 (2006).
[14] G. T. Moore, J. Math. Phys. **11**, 2679 (1970); S. A. Fulling and P. C. W. Davies, Proc. R. Soc. A **348**, 393 (1976); P. C. Davies and S. A. Fulling, Proc. R. Soc. A **356**, 237 (1977).
[15] G. Barton and C. Eberlein, Ann. Phys. (N.Y.) **227**, 222 (1993); M. Kardar and R. Golestanian, Rev. Mod. Phys. **71**, 1233 (1999); V. V. Dodonov, Modern Nonlinear Optics, Advances in Chemical Physics, edited by M. W. Evans (Wiley, New York, 2001), Part 3, Vol. **119**, p. 309.
[16] C. M. Wilson, G. Johansson, A. Pourkabirian, M. Simoen, J. R. Johansson, T. Duty, F. Nori, and P. Delsing, Nature (London) **479**, 376 (2011); P. Lahteenmaki, G. S. Paraoanu, J. Hassel, and P. J. Hakonen, Proc. Natl. Acad. Sci. U.S.A. **110**, 4234 (2013).
[17] T. H. Hansson, V. Oganesyan, and S. L. Sondhi, Ann. Phys. (Amsterdam) **313**, 497 (2004).
[18] A. R. Zhitnitsky, Ann. Phys. (Amsterdam) **336**, 462 (2013).
[19] K. T. Chen and P. A. Lee, Phys. Rev. B **83**, 125119 (2011).
[20] M. A. Shifman, *Advanced Topics in Quantum Field Theory: A Lecture Course* (Cambridge University Press, Cambridge, England, 2012).
[21] E. Witten, Ann. Phys. (N.Y.) **128**, 363 (1980).
[22] E. Witten, Phys. Rev. Lett. **81**, 2862 (1998).
[23] A. Bhoonah, E. Thomas, and A. R. Zhitnitsky, Nucl. Phys. **B890**, 30 (2014).
[24] A. Bienfait *et al.*, Nature (London) **531**, 74 (2016).
[25] V. Chandrasekhar, R. A. Webb, M. J. Brady, M. B. Ketchen, W. J. Gallagher, and A. Kleinsasser, Phys. Rev. Lett. **67**, 3578 (1991).
[26] G. Bressi, G. Carugno, R. Onofrio, and G. Ruoso, Phys. Rev. Lett. **88**, 041804 (2002).
[27] S. K. Lamoreaux, Phys. Rev. Lett. **78**, 5 (1997).
[28] A. Noguchi, Y. Shikano, K. Toyoda, and S. Urabe, Nat. Commun. **5**, 3868 (2014).
[29] A. Behtash, G. V. Dunne, T. Schaefer, T. Sulejmanpasic, and M. Unsal, arXiv:1510.03435.
[30] G. V. Dunne and M. Unsal, Annu. Rev. Nucl. Part. Sci. **66**, 245 (2016).
[31] Y. Tanizaki and T. Koike, Ann. Phys. (Amsterdam) **351**, 250 (2014).
[32] A. Cherman and M. Unsal, arXiv:1408.0012.
[33] A. Behtash, G. V. Dunne, T. Schaefer, T. Sulejmanpasic, and M. Unsal, Phys. Rev. Lett. **116**, 011601 (2016).
[34] A. R. Zhitnitsky, Phys. Rev. D **89**, 063529 (2014).
[35] A. R. Zhitnitsky, Phys. Rev. D **90**, 043504 (2014).
[36] A. R. Zhitnitsky, Phys. Rev. D **92**, 043512 (2015).
[37] N. S. Manton, Ann. Phys. (N.Y.) **159**, 220 (1985); R. Linares, L. F. Urrutia, and J. D. Vergara, arXiv:hep-th/0010114.